17 GHz OVERMODED DIELECTRIC PHOTONIC BAND GAP ACCELERATOR CAVITY*

Alan M. Cook†, Brian Munroe, Michael A. Shapiro, and Richard J. Temkin
Plasma Science and Fusion Center, MIT, Cambridge, MA, 02139, USA

Abstract

We present the design of an overmoded photonic band gap (PBG) accelerator cavity, made from a 2D lattice of sapphire rods supported between copper plates, that operates in a TM_{02}-like mode at 17 GHz. The cavity does not support the lower-frequency TM_{01}-like mode. Higher-order modes are damped effectively by removing rods from the lattice so that only the operating mode is supported with a high quality factor. The TM_{02} cavity mitigates the high pulsed heating of the copper surface seen in some metal-rod TM_{01} PBG cavities, which may be an advantage for high-gradient operation. We discuss plans for testing a 17 GHz TM_{02} standing-wave cavity at gradients above 100 MV/m.

INTRODUCTION

Microwave cavities based on photonic band gap (PBG) lattices are promising candidates for high-gradient accelerators because of their frequency selectivity; the operating mode resonates in the cavity, while parasitic wakefields radiate out through the lattice [1]. PBG accelerator cavities are typically formed by a lattice of metal or dielectric rods, with a single rod removed in the center to form a defect that confines an accelerating mode at a frequency within the band gap [2, 3]. The accelerating mode is similar to the TM_{01} mode of a disk-loaded waveguide (DLW) cavity. The mode is confined longitudinally by metal end plates with iris holes, which can be stacked to create a multiple-cell traveling-wave accelerator. Acceleration of an electron beam at a gradient of 35 MV/m has been demonstrated in a 17 GHz traveling-wave structure [4]. Wakefield measurements and high-power breakdown testing at 100 MV/m gradient have been performed [5, 6, 7, 8]. Current research also addresses laser-powered acceleration in optical PBG structures [9, 10].

In this paper, we study a PBG cavity made of a sapphire-rod lattice between copper plates using the commercial electromagnetic solver HFSS. The cavity is overmoded, operating in a TM_{02}-like mode, without competition from the lower-frequency TM_{01} mode. In the first section, we use 2D eigenmode simulations to study a cross-section of the cavity. These simulations explore the transverse confinement of modes in the defect region by the lattice, showing that the operating mode is the only high-Q mode supported by the cavity. In the second section, we use 3D eigenmode simulations to study the mode fields and power requirements of a single standing-wave cavity supporting a peak accelerating field of 200 MV/m. We find that the TM_{02} cavity mitigates the high pulsed heating of the copper surface seen in some metal-rod TM_{01} PBG cavities, which may be an advantage for high-gradient operation.

CAVITY MODES

A cross section of the overmoded cavity is shown in Fig. 1a, and the TM_{02}-like accelerating mode is shown in Fig. 1b. The arrangement of the rods is based on an equilateral triangle lattice with rod radius a and rod spacing b. The center rod and three concentric hexagonal rows of rods are removed from the bulk lattice to form the defect region. Rods are then removed in single-file rows extending from the defect, for the purpose of damping higher-order modes (HOMs). The filling factor a/b is fixed at 0.35, and the rod size is scaled so that the frequency of the TM_{02}-like mode is 17 GHz. $a/b = 0.35$ is chosen because no lower-order modes exist in the defect, and only two HOMs exist, at this value.

The radiative quality factor Q_{rad} quantifies the radia-

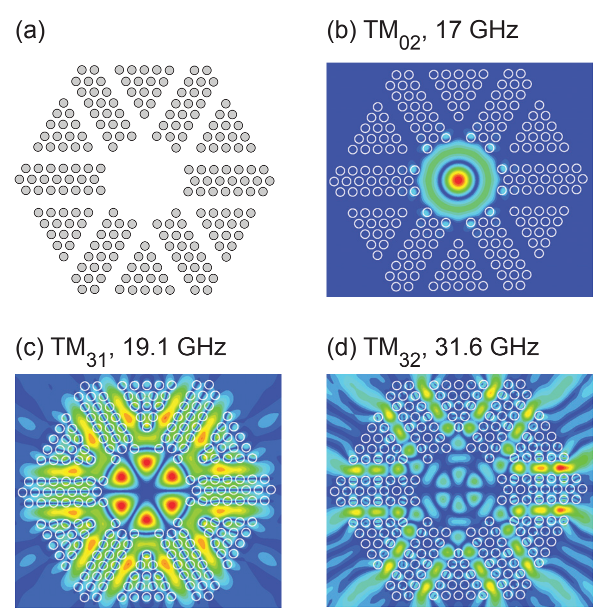

Figure 1: (a) Cross-section of TM_{02} cavity, showing dielectric rod arrangement. (b) TM_{02}-like operating mode at 17 GHz (E field complex magnitude). (c),(d) HOMs radiating out of lattice.

* Work supported by US Department of Energy, Office of High Energy Physics.

† alancook@mit.edu

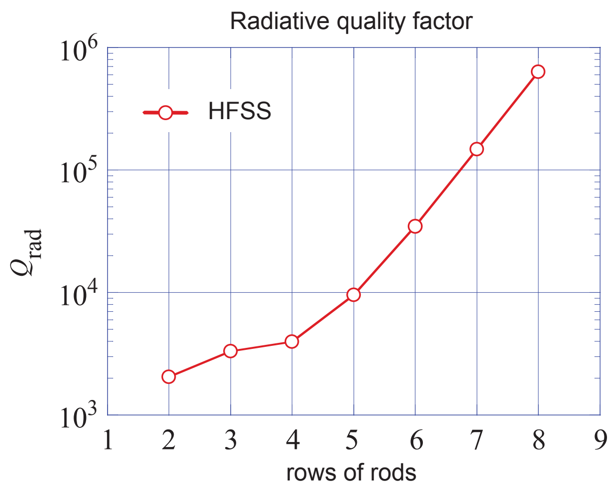

Figure 2: Radiative quality factor Q_{rad} of the TM_{02}-like mode as a function of concentric rows of rods comprising the cavity; calculated in HFSS.

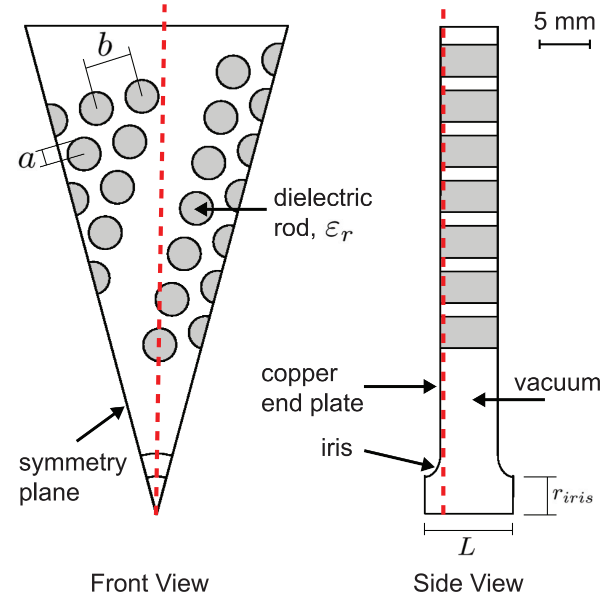

Figure 3: TM_{02} cavity model used in 3D eigenmode simulations.

tion loss out the open cavity wall. Q_{rad} is calculated in HFSS by turning off ohmic and dielectric losses and using a perfectly-matched layer at the boundary to allow radiation to escape. The HOMs (Fig. 1c,d) have very low radiative quality factors, due to the radial damping channels. The TM_{31}-like mode (Fig. 1c) has $Q_{rad} \approx 600$, while the TM_{32}-like mode has $Q_{rad} \approx 50$. Figure 2 shows Q_{rad} of the TM_{02}-like mode as a function of the number of concentric rows of rods making up the lattice. With several rows of rods, Q_{rad} is high enough that the total Q of the cavity will be dominated by ohmic losses.

MODE FIELDS AT HIGH GRADIENT

Figure 3 illustrates the HFSS model of a single cavity in a multi-cell structure used in 3D eigenmode simulations. The sapphire rods are supported between copper plates, and elliptically contoured irises couple the wave to adjacent cavities and allow beam clearance. A 30-degree wedge of the full cavity is simulated using symmetry planes, and a 180-degree phase shift is enforced between the entrance and exit irises to simulate a π-mode standing wave.

The effective accelerating gradient E_G is calculated by integrating the on-axis longitudinal field E_z over the cavity length L, accounting for the spatial and temporal field variation:

$$E_G = \frac{1}{L}\int_{-L/2}^{L/2} E_z cos(\omega z/c) dz. \quad (1)$$

The effective shunt impedance per unit length R_s, which quantifies the input power P_{in} required to drive a given gradient in the cavity, is given by [11]

$$R_s = \frac{E_G^2 L}{P_{in}}. \quad (2)$$

The Q factors associated with ohmic, dielectric, and radiation losses are calculated individually by running simulations with the other loss mechanisms turned off.

Table 1 compares the 17 GHz TM_{02} cavity with a conventional TM_{01} disk-loaded waveguide having identical iris geometry. The effective radius (r_{cav}) of the TM_{02} cavity defect region is approximately twice the radius of the DLW cavity. The shunt impedance is affected by the amount of energy stored in the cavity for a given gradient, and by the cavity Q. The disk-loaded waveguide cavity has a higher R_s than the TM_{02} cavity, due to its smaller size. The TM_{02} cavity has a higher total Q. Q_{tot} in each cavity is dominated by ohmic losses; dielectric and radiation losses, with Qs on the order of 10^5, have a small effect on Q_{tot} in the TM_{02} cavity.

Table 1: Standing-wave Cavity Parameters

	TM_{01} DLW	TM_{02} PBG
$\omega/2\pi$ (GHz)	17.14	17.14
r_{iris} (mm)	3.76	3.76
r_{cav} (mm)	7.71	≈ 16.28
L (mm)	8.74	8.74
a (mm)	—	1.65
b (mm)	—	4.7
ε_r	—	9.3
tan δ	—	3×10^{-5}
Q_{tot}	7150	1.0×10^4
Q_{ohm}	7150	1.2×10^4
Q_{diel}	—	1.3×10^5
Q_{rad}	—	1.3×10^5
R_s (MΩ/m)	65	30
E_G (MV/m)	$86.2\sqrt{P_{in}[MW]}$	$58.5\sqrt{P_{in}[MW]}$

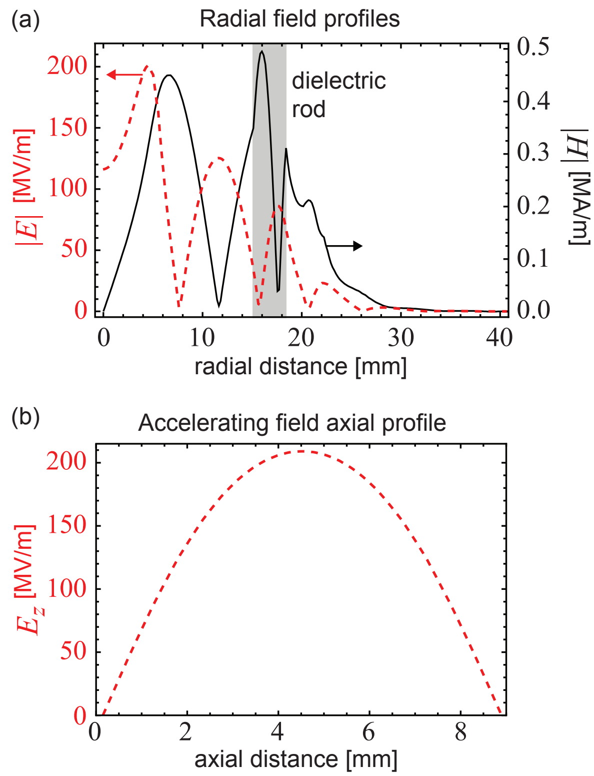

Figure 4: Cavity fields at $E_G = 100$ MV/m. (a) Radial profiles of complex magnitude of E (dashed red, left axis) and H (solid black, right axis). (b) Axial profile of accelerating field E_z.

Figure 4 shows the radial profiles of the E and H fields and the axial profile of E_z in the TM_{02} cavity, with the field magnitude corresponding to an accelerating gradient E_G = 100 MV/m. The profiles in Fig. 4a are plotted on a radius extending from the longitudinal axis, along the copper end plate surface, and bisecting the innermost rod, as shown by the dashed red lines in Fig. 3. Near the center of the cavity, $<$ 8 mm radial distance, the radial profiles are identical to those of the disk-loaded waveguide at the same gradient. The peak H field on the copper surface is $\sim$ 500 kA/m (Fig. 4a), similar to the peak H field in the disk-loaded structure. For comparison, in a 17 GHz TM_{01} PBG structure with circular metal rods, the peak H field at the inner rods reaches $\sim$ 900 kA/m for a 100 MV/m gradient [12]. The TM_{02} cavity may an advantage in terms of lower pulsed heating of the copper surface, which is proportional to H^2 [13].

CONCLUSION

We have used electromagnetic simulations to study a sapphire-rod photonic band gap accelerator cavity operating in a TM_{02}-like mode at 17 GHz. The operating mode is the only mode supported by the cavity with a high radiative Q. The peak magnetic field on the copper end plates is similar to that in a TM_{01} disk-loaded waveguide cavity, and significantly lower than in a TM_{01} PBG cavity with circular copper rods. This is desirable for operation at high gradient, where pulsed heating of the copper surface is known to be a factor in microwave vacuum breakdown.

We plan to test a prototype of this cavity under high power at the MIT 17 GHz accelerator facility (see [12], these proceedings). A 17 GHz klystron (Haimson Research Corporation) will provide up to 4 MW of microwave power to a test stand. The cavity design presented here can achieve a gradient of $E_G = 100$ MV/m at an input power level $P_{in} = 2.9$ MW (Table 1, last row). Testing the TM_{02} PBG structure at high power will reveal interesting information about vacuum breakdown on copper/dielectric interfaces at high microwave frequencies.

REFERENCES

[1] N. Kroll, D. R. Smith, and S. Schultz, in *AIP Conference Proceedings Vol. 279, Advanced Accelerator Concepts Workshop* (1992) pp. 197–211

[2] M. A. Shapiro, W. J. Brown, I. Mastovsky, J. R. Sirigiri, and R. J. Temkin, Phys. Rev. ST Accel. Beams **4**, 042001 (2001)

[3] M. R. Masullo, A. Andreone, E. D. Gennaro, S. Albanese, F. Francomacaro, M. Panniello, V. G. Vaccaro, and G. Lamura, Microwave and Optical Technology Letters **48**, 2486 (2006)

[4] E. I. Smirnova, A. S. Kesar, I. Mastovsky, M. A. Shapiro, and R. J. Temkin, Phys. Rev. Lett. **95**, 074801 (2005)

[5] R. A. Marsh, M. A. Shapiro, and R. J. Temkin, in *Proceedings of 2008 European Particle Accelerator Conference* (2008)

[6] R. A. Marsh, M. A. Shapiro, R. J. Temkin, E. I. Smirnova, and J. F. DeFord., Nucl. Instr. and Meth. A **618**, 16 (2010)

[7] C. Jing, F. Gao, S. Antipov, Z. Yusof, M. Conde, J. G. Power, P. Xu, S. Zheng, H. Chen, C. Tang, and W. Gai, Phys. Rev. ST Accel. Beams **12**, 121302 (2009)

[8] R. A. Marsh, M. A. Shapiro, R. J. Temkin, V. A. Dolgashev, L. L. Laurent, J. R. Lewandowski, A. D. Yeremian, and S. G. Tantawi, Phys. Rev. ST Accel. Beams **14**, 021301 (2011)

[9] B. Cowan, Phys. Rev. ST Accel. Beams **11**, 011301 (2008)

[10] C.-K. Ng, R. J. England, L.-Q. Lee, R. Noble, V. Rawat, and J. Spencer, Phys. Rev. ST Accel. Beams **13**, 121301 (2010)

[11] T. Wangler, *RF Linear Accelerators* (Wiley-Interscience, 1998) pp. 345–353

[12] B. J. Munroe, M. A. Shapiro, R. J. Temkin, R. A. Marsh, V. Dolgashev, and S. G. Tantawi, in *PAC 2011 Proceedings* (2011)

[13] P. B. Wilson, AIP Conf. Proc. **397**, 191 (1997)